Title
Reaction of Chlorine Molecules with Unsaturated Submicron Organic Particles

Journal
Zeitschrift für Physikalische Chemie, 229(10-12)

ISSN
0942-9352

Authors
Popolan-Vaida, Denisia M
Liu, Chen-Lin
Nah, Theodora
et al.

Publication Date
2015-10-28

DOI
10.1515/zpch-2015-0662

Peer reviewed

Denisia M. Popolan-Vaida, Chen-Lin Liu, Theodora Nah,
Kevin R. Wilson, and Stephen R. Leone*

Reaction of Chlorine Molecules with Unsaturated Submicron Organic Particles

DOI 10.1515/zpch-2015-0662
Received July 21, 2014; accepted August 4, 2014

Abstract: The reaction of closed shell Cl_2 molecules with sub-micron droplets composed of unsaturated molecules, oleic acid (OA), linoleic acid (LA), linolenic acid (LNA), or squalene (Sqe), are investigated in an atmospheric pressure flow tube reactor in conjunction with a vacuum ultraviolet photoionization aerosol mass spectrometer and a scanning mobility particle sizer. Cl_2 is found to react with all particles, and the reactive uptake coefficients depend on the number of unsaturated reaction sites, e.g., $\gamma_{Cl_2}^{Sqe} = (0.66 \pm 0.03) \times 10^{-4}$ versus $\gamma_{Cl_2}^{OA} = (0.23 \pm 0.01) \times 10^{-4}$. In addition, the chemical evolution of squalene and its chlorinated products reveal that the reaction becomes slower for higher chlorinated products.

Keywords: Reaction Kinetics, Reactive Uptake Coefficient, Aerosols, Unsaturated Fatty Acids, Squalene.

Dedicated to Prof. Dr. Dr. h.c. mult. Jürgen Troe on the occasion of his 75th birthday

***Corresponding author: Stephen R. Leone,** Department of Chemistry, University of California, Berkeley, CA 94720, United States; and Department of Physics, University of California, Berkeley, CA 94720, United States; and Chemical Sciences Division, Lawrence Berkeley National Laboratory, Berkeley, CA 94720, United States, e-mail: srl@berkeley.edu
Kevin R. Wilson: Chemical Sciences Division, Lawrence Berkeley National Laboratory, Berkeley, CA 94720, United States
Denisia M. Popolan-Vaida, Theodora Nah: Chemical Sciences Division, Lawrence Berkeley National Laboratory, Berkeley, CA 94720, United States; and Department of Chemistry, University of California, Berkeley, CA 94720, United States
Chen-Lin Liu: Chemical Sciences Division, Lawrence Berkeley National Laboratory, Berkeley, CA 94720, United States; and Department of Chemistry, University of California, Berkeley, CA 94720, United States; and Scientific Research Division, National Synchrotron Radiation Research Center, Hsinchu 30076, Taiwan

1 Introduction

A great deal of research has been devoted to understand Cl atom chemistry in the atmosphere, motivated in part due to their contribution to the depletion of stratospheric ozone [1–3]. In addition, Cl atoms are assumed to play an important role in tropospheric hydrocarbon chemistry, especially in the marine boundary layer [4, 5], the Arctic region [6, 7], and industrialized coastal areas [8]. Spicer et al. showed that the role of Cl-initiated oxidation might be comparably important to OH-initiated oxidation in coastal and industrialized areas although the global chlorine concentration is considerably lower than that of OH [8].

In contrast, less attention has been dedicated to understanding atmospheric Cl_2 heterogeneous chemistry, although high levels of Cl_2 have been observed in the Atlantic marine boundary layer (up to 35 pptv at night [9] and up to 400 pptv at early morning and late afternoon [10]) and in polluted coastal areas (up to 150 pptv at night [8, 11]). The origin of Cl_2 in the atmosphere can be associated with multiple sources. For example, Cl_2 can originate from anthropogenic sources as a result of oil and metal refining, industrial processes linked with power generation, or large-scale bleaching processes at water treatment plants [12]. Cl_2 can also be formed in situ in the atmosphere through a single-step [13] or multi-step [14–18] reactions of chloride-containing aerosol particles resulting in a buildup of Cl_2 especially during the night.

Organic material, which comprises a significant fraction (20% – 90%) of the total fine aerosol mass in the lower troposphere [19], can be readily oxidized through heterogeneous reactions by gas-phase radicals or molecules. In this context, details about the heterogeneous reactions between atmospheric oxidants and organic aerosols are of great importance and will help to understand the fate of organic aerosols in the atmosphere.

The atmospheric concentrations of alkenes are drastically impacted by both anthropogenic and biogenic emissions. Alkenes can be found in a variety of fuels and automobile exhaust, as well as in other industrial and agricultural (biomass burning) processes [20, 21]. Biogenic sources of alkenes include emissions from vegetation, soils and the ocean [22]. On the other hand, fatty acids represent some of the most common components found in ambient fine particles originating from multiple sources such as meat cooking, road dust, leaf abrasion and tire wear [23, 24].

In general, the course of reaction between Cl_2 molecules and alkenes can proceed through several reaction mechanisms. The addition of a chlorine molecule to the double bond of alkenes can be followed by two mechanisms: (i) a single-step mechanism, called addition mechanism, in which the two chlorine atoms at-

tach to the p-orbitals of the C=C double bond as the Cl–Cl bond breaks to yield only the *cis* product, and (ii) a two-step mechanism, called a polar mechanism, in which the Cl–Cl bond is broken heterolytically and carbonium ion intermediates occur, resulting in the formation of *cis* as well as *trans* products. Alkenes bearing a side-chain on the double bond can react (iii) through a substitutive mechanism in which the double bond remains intact while substitution of allylic hydrogen atoms by chlorine atoms takes place.

The reactions between Cl_2 molecules and a variety of alkenes have been investigated under various experimental conditions, and factors such as temperature, reaction medium, solvent, structure of alkenes, and polarity of the electrophile are found to significantly affect the product distribution and the kinetics of these reactions.

The reactions of Cl_2 with alkenes in the liquid phase or in aqueous and organic solutions at ambient or slightly elevated temperature are well-characterized and known to result in the formation of mainly dichloroalkanes as a result of Cl_2 addition to the double bond of alkenes. The reactions are found to proceed either by the addition mechanism (i) or in the case of a polar solvent by the polar mechanism (ii) [25]. However, as the reaction temperature is increased, typically to 400–500 °C, the substitution reaction (iii) with retention of the double bond begins and becomes more prominent. The ambient temperature reaction between Cl_2 and alkenes bearing a side-chain on the double bond, such as iso-butene and other tertiary alkenes, are reported to undergo substitution exclusively, the double bond being retained as such [26].

Many data suggest that simple alkenes and chlorine react slowly, if at all, in the gas-phase at ambient temperature while the primary product is generally the dichloroalkanes [27, 28]. With increasing temperature, the gas-phase reaction between alkenes and Cl_2 also begins to proceed through a substitutive mechanism [26].

Graham et al. reported the ice-catalyzed reaction of Cl_2 with propene (C_3H_6) [29]. The reaction is observed to proceed by Cl_2 addition to the C=C double bond of propene and formation of 1,2-dichloropropane. The results suggest a heterogeneous sink for Cl_2 in the stratosphere.

Compared to the gas-phase, there are potentially more highly coupled reactions taking place between reactants, products, and intermediates in case of heterogeneous reactions. As a consequence, reactions that normally have low probability in the gas-phase are found to have an enhanced surface reaction probability [30].

The reaction of Cl_2 with submicron organic particles composed of unsaturated organic molecules has not been investigated. This work considers the kinetics and product formation of the heterogeneous reaction of Cl_2 molecules with

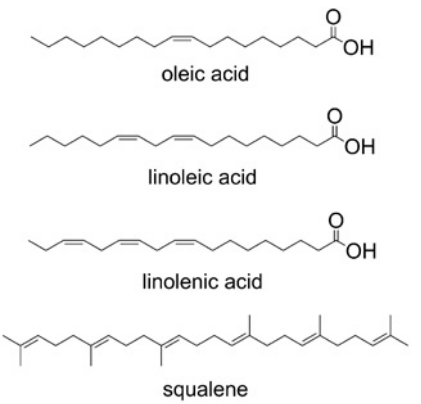

Figure 1: Chemical structure of oleic acid, linoleic acid, linolenic acid and squalene, respectively.

unsaturated particles composed of Sqe, OA, LA or LNA. Sqe is a liquid branched alkene with 6 C=C double bonds, while the unsaturated fatty acids (UFAs) OA, LA, and LNA are liquid linear carboxylic acids with 1, 2, and 3 C=C double bonds, respectively. The molecular structures of unsaturated fatty acids and Sqe are shown in Figure 1.

The reactions of squalene and unsaturated fatty acid particles with a variety of gas-phase species, such as OH, NO_3, O_3, and I have been already investigated, as noted next. The kinetics and products of the heterogeneous OH-initiated oxidation of Sqe particles have been measured in this laboratory and compared with the OH initiated oxidation of UFA particles (OA, LA, and LNA) to understand the influence of molecular structure (branched vs linear) and chemical functionality (alkene vs carboxylic acid) on the reaction rates and mechanism [31, 32]. The reactive uptake coefficients of NO_3 by submicron particles containing Sqe or UFAs have been investigated as model systems to understand the atmospheric implications of the heterogeneous chemical processes involving NO_3 [33, 34]. The ozonolysis of UFA particles has been measured and compared [35–38]. The probability of heterogeneous reaction between O_3 and UFAs are found to be enhanced with respect to the reaction of O_3 with alkenes in the gas-phase.

The reaction of iodine atoms with Sqe particles has also been recently investigated in this group and compared with the reaction between I atoms and saturated squalane particles [39]. The reaction of I atoms with Sqe particles results in iodinated products and is found to have a reactive uptake probability of 10^{-4}, although the gas-phase reaction of iodine atoms with hydrocarbon molecules is known to be energetically unfavorable.

The heterogeneous reaction of Cl_2 molecules with submicron droplets composed of unsaturated molecules such as OA, LA, LNA or Sqe is investigated here in an atmospheric pressure flow tube reactor with a vacuum ultraviolet time-of-

flight aerosol mass spectrometer (VUV-AMS) and scanning mobility particle sizer (SMPS). These systems represent models for heterogeneous interfacial chemistry between a closed shell molecule and unsaturated organic particles. The present work is designed to understand the heterogeneous kinetics and chemical mechanism of the Cl_2-initiated reaction with unsaturated organic particles as a function of the number of C=C double bonds in the unsaturated molecule that compose the particles, specifically by monitoring the evolution of the reactive uptake coefficients as a function of particle degree of unsaturation (number of C=C double bonds in the molecule that compose the particles). These reactions are expected to proceed by an addition mechanism in which the Cl_2 molecule attacks the C=C double bonds present in the molecules that compose the unsaturated particles.

2 Methods

2.1 Experimental setup

The experiments are carried out in an atmospheric pressure flow tube reactor system schematically displayed in Figure 2. Details of the experimental setup have been given elsewhere [40]. Briefly, the particles are formed by homogeneous nucleation of the organic vapor in a N_2 stream flowing through a ~ 45 cm long Pyrex tube containing liquid samples of squalene, linolenic acid, linoleic acid, or oleic acid. The Pyrex tube is heated in a tube furnace to well-defined temperatures to produce a log-normal particle size distribution with a mean surface-weighted diameter between 120 nm to 170 nm. 80.5 ppm Cl_2 is mixed with the aerosol stream in a balance of atmospheric pressure N_2 prior to admission into the flow tube reactor. The mixed gases and particles are then introduced into a 130 cm long, 2.5 cm inner diameter type 219 quartz reactor. The total flow rate through the flow tube is fixed at 0.7 – 1.5 SLM (standard liter per minute) depending on the required Cl_2 exposure, which corresponds to a reaction time of around 30 to 56 s. All experiments reported here are performed in an O_2 free environment.

The flow exiting the reactor is passed through a small column packed with potassium carbonate (Cl_2 scrubber) to remove Cl_2 and prevent propagation of the reaction beyond the flow tube. Subsequently, a part of the flow is sampled into a custom built vacuum ultraviolet aerosol mass spectrometer (VUV-AMS) to extract information about the chemical composition of the reacted particles. The VUV-AMS measures the aerosol composition by thermally vaporizing the aerosol (~ 100 °C) followed by tunable VUV photoionization. For the experiments re-

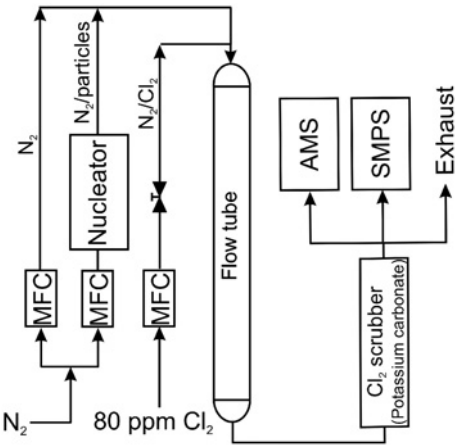

Figure 2: Schematic representation of the experimental setup employed to investigate the heterogeneous reaction of squalene (Sqe) and unsaturated fatty acids (OA, LA and LNA) particles with Cl_2. The total flow rate through the flow tube reactor is regulated by calibrated MFCs (mass flow controllers). After reaction, the gas stream is sampled by a SMPS (scanning mobility particle sizer) and VUV-AMS (vacuum ultraviolet aerosol mass spectrometer) in order to measure the particle size distribution and aerosol composition.

ported here, the droplets are vaporized and photoionized by 9.5 eV radiation produced by the Chemical Dynamics Beamline at the Advanced Light Source.

Part of the flow exiting the reactor, not sampled by the VUV-AMS, is sent to a scanning mobility particle sizer (SMPS, TSI model 3936) to simultaneously measure particle size distribution and number concentration.

2.2 Data evaluation

The rate constant for the heterogeneous reaction of unsaturated particles (UP), k_{UP} (here UP = squalene, oleic acid, linoleic acid, and linolenic acid) with Cl_2 is quantified by measuring the decay in the relative intensities of the unsaturated particle ion signals in the mass spectrum as a function of Cl_2 exposure. The rate constant (k_{UP}) for the Cl_2 reaction of unsaturated particles is determined using the standard relative rate method described by Smith et al. [40], which probes the disappearance of particles.

$$\frac{[UP]}{[UP]_0} = \exp(-k_{UP} \cdot [Cl_2] \cdot t) \tag{1}$$

where [UP] and $[UP]_0$ are the final and initial unsaturated particle concentrations, respectively. $[Cl_2]$ represents the concentration of gas-phase Cl_2 molecules in the flow reactor, while t is the reaction time that can be determined by dividing the flow volume by the flow rate.

Assuming the reaction occurs heterogeneously, an effective reactive uptake coefficient ($\gamma_{Cl_2}^{UP}$) can be defined as the fraction of chlorine molecules colliding

with unsaturated particles heterogeneously that results in a reaction. Using the formalism, originally developed by Smith et al. [40] for the reaction of squalane with OH, the reaction probability can be written in our case as follows,

$$\gamma_{Cl_2}^{UP} = \frac{4 \cdot k_{UP} \cdot D_{surf} \cdot \rho_0 \cdot N_A}{6 \cdot \bar{c} \cdot M_{UP}} \quad (2)$$

where D_{surf} is the mean surface-weighted particle diameter, ρ_0 is the initial compound density ($0.858\ g \cdot cm^{-3}$ for squalene, $0.9157\ g \cdot cm^{-3}$ for linolenic acid, $0.9\ g \cdot cm^{-3}$ for linoleic acid, and $0.895\ g \cdot cm^{-3}$ for oleic acid, respectively), N_A is Avogadro's number, $\bar{c}$ is the mean speed of gas-phase Cl_2, while the values of M_{UP} are the molar masses of unsaturated particles, equal to 410.72 g/mole for Sqe, 278.43 g/mole for LNA, 280.45 g/mole for LA, and 282.46 g/mole for OA, respectively.

As the reaction evolves the particle composition changes from pure particle to greater chlorinated species. A direct comparison of the unsaturated squalene particle reaction probability ($\gamma_{Cl_2}^{UP}$) with that of subsequent products, (i.e. $\gamma_{Cl_2}^{(UP-nH)Cl_n}$) is performed systematically in order to draw a more general conclusion about how the reactive effective uptake coefficient changes as the reaction proceeds and the particle is chemically transformed.

3 Results and discussion

The present study focuses first on the reaction products and kinetics of squalene $+Cl_2$ reaction (Section 3.1). The reactions between Cl_2 and unsaturated fatty acids particles are presented in Section 3.2, and the reactive uptake values are calculated and compared, in Section 3.3.

3.1 Reaction of Cl_2 with submicron squalene particles

Squalene (Sqe, $C_{30}H_{50}$) is a branched alkene that has six C=C double bonds and contains 8 primary, 16 secondary, and 6 tertiary carbon atoms. Sqe represents an ideal model system to mimic the variety of reactive carbon sites typically found on hydrocarbon surfaces and that may also occur in ambient organic aerosols.

Figure 3 displays the 9.5 eV photoionization mass spectra of squalene (a) before and (b) after Cl_2 exposure. No peaks with masses higher than squalene are observed in the absence of Cl_2, see Figure 3(a). When Cl_2 is added into the flow tube, the squalene peak decreases and is accompanied by the formation of higher molecular weight products as observed in the aerosol mass spectrum. The number

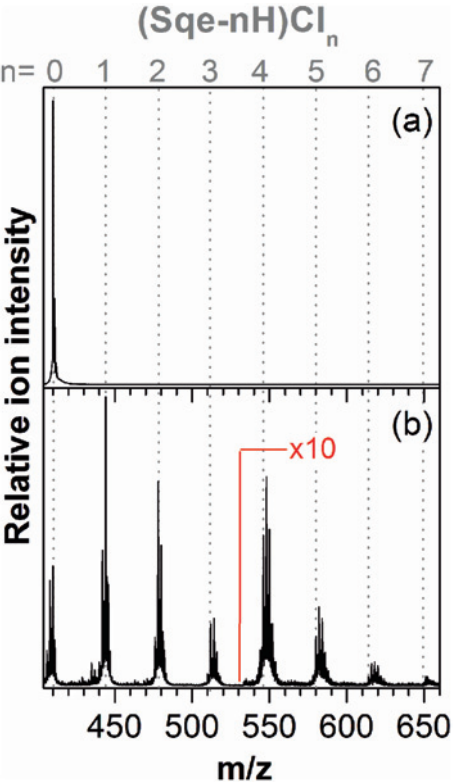

Figure 3: The VUV photoionization mass spectra of squalene (Sqe) particles recorded at a photoionization energy of 9.5 eV: (a) before and (b) after the exposure to Cl_2 molecule (5.75×10^{16} s · molec. · cm^{-3}). Note that the region of the mass spectrum above $m/z = 530$ in panel (b) is multiplied by a factor of 10.

of chlorinated products formed during the reaction is observed to increase with increasing Cl_2 exposure. As can be seen in Figure 3(b), up to seven groups of higher molecular weight masses, separated by 34 amu, are observed for the highest Cl_2 exposure measured in the present experiment. Based on the mass difference from the squalene molecular ion peak to the higher molecular weight product peaks observed in the experiment, the newly formed peaks appear to correspond to products in which a H atom(s) is(are) replaced by Cl atom(s) for each reaction. For simplicity, these products are further referred to as (Sqe – nH)Cl_n, where $n = 1$–7 designates the number of H atoms missing from the Sqe molecule and the number of Cl atoms added to the Sqe molecule, respectively. As fragmentation patterns and photoionization efficiency may depend on the identity of the neutral product molecules, it is difficult to draw any conclusion about absolute product yield based on the relative peak intensities in the product mass spectrum.

Similar to the reactions of alkenes with Cl_2 in the gas-phase [26, 27], we anticipate that the initial step of the ambient temperature heterogeneous reaction between Cl_2 and Sqe particles involves Cl_2 addition. Thus, two chlorine atoms

add to the p-orbitals of one of the squalene C=C double bonds as the Cl–Cl bond breaks to create an activated complex. The energized complex could undergo dissociation again or be stabilized by collisions. The larger the molecule, the longer lived will be the addition complex, favoring stabilization.

The formation of the ionic π-complex intermediates in halogen addition is unfavorable in this case due to the absence of polar solvent, and consequently the polar mechanism seems unlikely. As already mentioned, apart from the liquid-phase reactions where a substitutive mechanism was observed to be the initiation step in the room temperature chlorination of tertiary alkenes, in all the other cases the substitutive mechanism only starts playing a role when the reaction temperature is increased. Since the reaction between squalene particles and Cl_2 was investigated here under ambient temperature conditions, we anticipate that the substitutive mechanism should not play any role in the chlorination reaction. However, we cannot exclude the possibility that the substitutive reaction might become important once the chlorinated squalene products are formed, which might present a different reaction behavior from that of Sqe. Primarily, we consider that Cl_2 addition to C=C double bond is the most favorable reaction mechanism.

Within the signal-to-noise of the experiment, no products that correspond to the formation of $Sqe(Cl_2)_n$ (with $n = 1, 2, 3, \ldots$) are observed in the recorded product mass spectra. However, dissociative photoionization is a likely process for any $Sqe(Cl_2)_n$ addition products that are formed prior to the mass detection step. Dissociative photoionization has been observed to be the dominant process in a series of experiments performed in our laboratory where the reaction of Cl radical with submicron squalane droplets was investigated [41]. For smaller dichlorinated hydrocarbons, such as 1,2-dichloroethane, HCl elimination upon photoionization represents a significant dissociation pathway [42]. Furthermore, the electron impact mass spectra of small dichlorinated hydrocarbons produces hydrocarbon fragments consistent with HCl elimination, providing further evidence for this channel [43]. It is therefore very likely that a similar dissociative photoionization pathway occurs for the chlorinated addition products of squalene observed here, and for example, (Sqe – H)Cl ($m/z = 444$) may be the fingerprint of the $SqeCl_2$ ($m/z = 480$) molecule, which undergoes dissociative photoionization and eliminates HCl. In this context, what appears to be reaction products in which a H atom(s) is(are) replaced by a Cl atom(s) for each reaction is likely the fingerprint for the next dichloro addition species that is dissociatively ionized.

Apart from the $(Sqe - nH)Cl_n$ chlorinated products, peaks with two mass units smaller than the $(Sqe - nH)Cl_n$ products are also observed in the mass spectrum (Figure 3b). These peaks can be attributed to species in which not just one HCl molecule, but multiple HCl molecules are eliminated from neutral species in order to reach a final product after the formation of energetically

unstable highly chlorinated squalene species ($Sqe(Cl_2)_n$, $n = 2, 3, 4, \ldots$). Moreover, a HCl molecule can also be eliminated via dissociative photoionization of $(Sqe - nH)Cl_n$ during the photoionization step. In this case, the $Sqe - 2H^+$ peak forms from the elimination of two HCl molecules from the $SqeCl_2$, possibly one in the neutral and one in the photoionization step, $(Sqe - 3H)Cl^+$ forms from the elimination of three HCl molecules from the $SqeCl_4$, and so on. In addition, $(Sqe - H)Cl^+$ and $Sqe - 2H^+$ are found to have a similar kinetic behavior suggesting that both $(Sqe - H)Cl^+$ and $Sqe - 2H^+$ ions may possibly originate from $SqeCl_2$. A similar behavior is observed for pairs of higher molecular weight species, such as $(Sqe - nH)Cl_n$ and $(Sqe - (n + 1)H)Cl_{n-1}$ with $n = 2, 3, 4, \ldots$ On the other hand, it is hard to draw a final conclusion based upon the observed similarities in the kinetic behavior of different product ions. The squalene + Cl_2 reaction proceeds through a very complex series of events and due to the time scale of the present experiment it is not certain that we are able to observe the elementary steps of this reaction. As a result several kinetic behaviors could look similar.

Furthermore, peaks with mass slightly higher than squalene, i.e., m/z = 411, 412, and its chlorinated products, i.e., m/z = 445, 446, 479, 480, etc. are also observed. The nature of these peaks can be explained by the natural isotopic abundance of ^{13}C and ^{37}Cl isotopes of squalene and its chlorinated products. The relative intensities of isotopic peaks are consistent with the carbon chain length given the instrumental uncertainty. The instrumental uncertainty is estimated on the basis of the background noise signal of the AMS (a maximum of 1 count per s) in the present experiment. Any variation in the ion peak intensity of $\leq 0.02\%$ is considered instrumental uncertainty.

The Cl_2 molecule appears to be unreactive towards saturated hydrocarbon particles. Previous reports from our laboratory, where Cl_2 was used as a precursor for Cl radical initiation reaction, revealed no evidence for product formation between saturated squalane particles and Cl_2, when no photolysis lamps were used (the lamps initiate the Cl radical formation) [41]. Squalane ($C_{30}H_{62}$) is a saturated hydrocarbon that has a similar structure to that of squalene investigated in these studies. Although the results observed in the case of squalane particles suggest that the Cl_2 molecule is essentially inert toward saturated bonds, the presence of the $C(sp^3)$–H bonds in the squalene structure that are allylic in character and, as a consequence, have a significant lower bond energy makes those bonds more reactive than their equivalent in squalane. Squalene has a total of 44 H atoms from $C(sp^3)$–H bonds that are allylic in nature, since they are attached to C atoms that are adjacent to C=C double bonds. Reaction of Cl_2 towards the allylic sites of squalene might be a reason why products that seem to require more than six Cl_2 additions are observed in the mass spectrum.

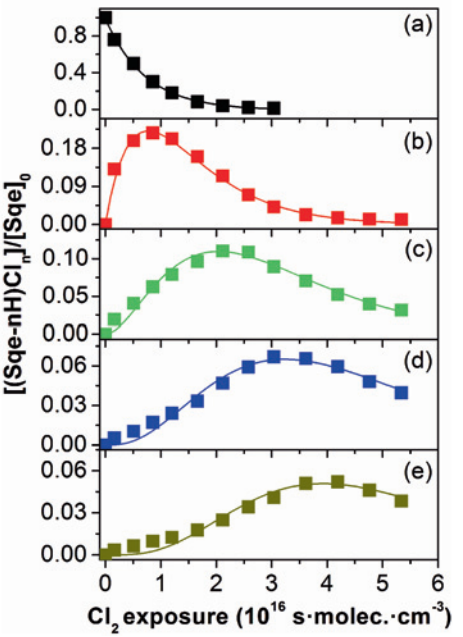

Figure 4: The kinetic evolution of (a) squalene (Sqe^+) and its first four generations of reaction products (b) $(Sqe - H)Cl^+$, (c) $(Sqe - 2H)Cl_2^+$, (d) $(Sqe - 3H)Cl_3^+$ and (e) $(Sqe - 4H)Cl_4^+$ represented as a function of Cl_2 exposure. The filled symbols represent the measured data while the solid lines are results of a sequential reaction model fit described in Section 3.3.

In summary, the experimental results suggest that the reaction most likely proceeds through an addition mechanism in which the Cl_2 molecules sequentially attack the six C=C double bonds of Sqe to form energetically unstable highly chlorinated squalene species $Sqe(Cl_2)_n^*$, which undergo further losses of HCl as follows:

$$\begin{aligned} Sqe + nCl_2 \rightarrow Sqe(Cl_2)_n^* &\xrightarrow{-q\mathrm{HCl}} (Sqe - m\mathrm{H})Cl_m + h\nu \\ &\rightarrow (Sqe - (m-1)\mathrm{H})Cl_{m-1}^+ + \mathrm{HCl}\,. \end{aligned}$$

This mechanism does not consider any structural changes or any changes in the reactivity that might occur after Cl_2 is added to the squalene molecules. In addition, we cannot exclude the existence of additional pathways or very fast intermediate steps that cannot be detected in the time scale of the present experiment.

In order to reveal new insights about the mechanism of Sqe reaction with Cl_2, kinetic measurements are also performed. In all experiments reported here, where kinetics are measured, the Cl_2 exposure is varied by keeping the flow rate (i.e. reaction time) constant and varying the Cl_2 concentration. Figure 4 displays the kinetic evolution of (a) Sqe^+ and its first four generation major chlorinated products, (b) $(Sqe - H)Cl^+$, (c) $(Sqe - 2H)Cl_2^+$, (d) $(Sqe - 3H)Cl_3^+$ and (e) $(Sqe - 4H)Cl_4^+$, as a function of Cl_2 exposure. As can be seen in Figure 4(b)–(e),

each product is both formed and decays over the course of the reaction. In addition, different reaction products arise at different Cl_2 exposures. Model fits to the (Sqe − H)Cl, (Sqe − 2H)Cl_2, (Sqe − 2H)Cl_3 and (Sqe − 2H)Cl_4 experimental data are displayed as solid lines in Figure 4(b), (c), (d), and (e), respectively. A detailed description of the fitting procedure is provided in Section 3.3.

3.2 Reaction of Cl_2 with linolenic acid, linoleic acis, and oleic acid particles

The single-component UFA particles investigated in the present study, i.e. oleic acid (OA, $C_{18}H_{34}O_2$), linoleic acid (LA, $C_{18}H_{32}O_2$), and linolenic acid (LNA, $C_{18}H_{30}O_2$), all have a similar backbone structure but with one, two, and three C=C double bonds, respectively. They represent model systems to investigate the role that multiple reactive sites have on controlling the heterogeneous reaction probability. In addition, the comparison between the Sqe particles and UFA particles might reveal the influence of chemical functionality (alkene vs carboxylic acids) on the heterogeneous reaction probability.

The 9.5 eV photoionization product mass spectra recorded after the reaction of LNA, LA, and OA with Cl_2 are displayed in Figure 5(a), (b), and (c), respectively. A close inspection of the recorded product mass spectra in Figure 5 reveals that the major products are similar to that of Sqe, i.e. the reaction products appear in groups of 6 to 7 peaks, generally separated by 34 amu, apart from the last group of product peaks of LNA, which is separated by 36 amu (see Figure 5a). In addition, the number of observed products for each UFA particle appears to match the number of C=C double bonds in the unsaturated fatty acid that compose the particles. For instance, the LNA product mass spectrum displayed in Figure 5(a) presents three clusters of product peaks, the first two being separated by 34 amu while the last one is separated by 36 amu. Based on the exact mass difference from the LNA molecular ion peak, the product peak at mass $m/z = 312$ corresponds to addition of a Cl_2 molecule to one of the double bonds of LNA followed by HCl elimination during ionization. This mechanism repeats for every double bond of LNA resulting in peaks in the mass spectrum that have the (LNA − nH)Cl_n configuration. However, as already mentioned above, the last group of peaks appear to be separated by 36 amu (see Figure 5a). This mass at $m/z = 382$ might correspond to the (LNA − H)Cl_3^+ ion formed as a result of dissociative photoionization of LNA$(Cl_2)_2$ that loses an HCl molecule. Groups of peaks separated by 36 amu were exclusively observed in the case of unsaturated LNA particles.

Similar to the case of squalene, the peaks in Figure 5(a) with two mass units smaller than the major products might be attributed to products in which multi-

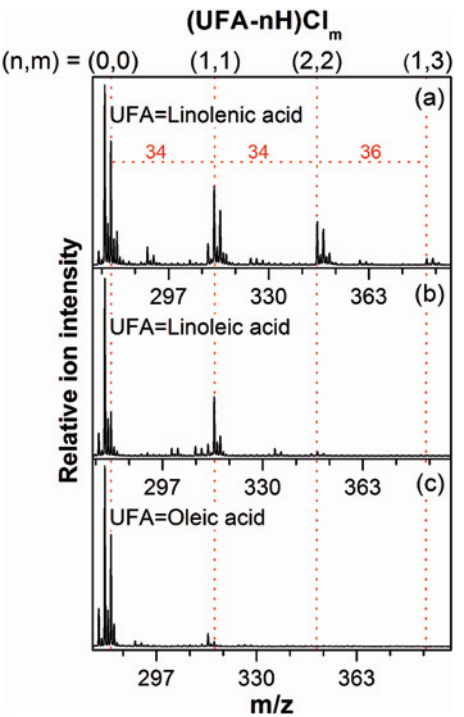

Figure 5: The VUV photoionization product mass spectra obtained after the reaction of Cl_2 with (a) linolenic acid droplets, (b) linoleic acid droplets and (c) oleic acid droplets, respectively. The mass spectra were recorded at a photoionization energy of 9.5 eV. The red insert shows the exact mass difference from the unsaturated fatty acid parent ion to the main peak in each group of reaction products.

ple HCl molecules are eliminated as a result of dissociative photoionization of the chlorinated parents. For instance, LNA $- 2H^+$ is the fingerprint of the $LNACl_2$ molecule that undergoes dissociative photoionization and eliminates two HCl molecules. Both, $(LNA - H)Cl^+$ and LNA $- 2H^+$ are observed to follow the same kinetic behavior, which suggests that both products originate from a $LNACl_2$ molecule that loses one and two HCl molecules during ionization.

In addition, groups of low intensity peaks with m/z = 290, 292, 324, 326, 328, 360 and 362 are also observed in the product mass spectrum of LNA (Figure 5a). These peaks follow the kinetic behavior of the higher molecular weight reaction products and consequently are attributed to their fragmentation produced during the ionization process. Similar mass spectra are also observed for linoleic acid (Figure 5b) and oleic acid (Figure 5c) particles after reaction with Cl_2 molecule.

As shown in Figure 1, the structure and the composition of UFAs are different from that of squalene molecule, i.e. UFAs have no tertiary carbons, but instead have a carboxylic acid functional group in their composition. In order to understand the carboxylic acid functional group contribution to the observed reactivity of the UFAs, the reaction of particles composed of stearic acid with Cl_2

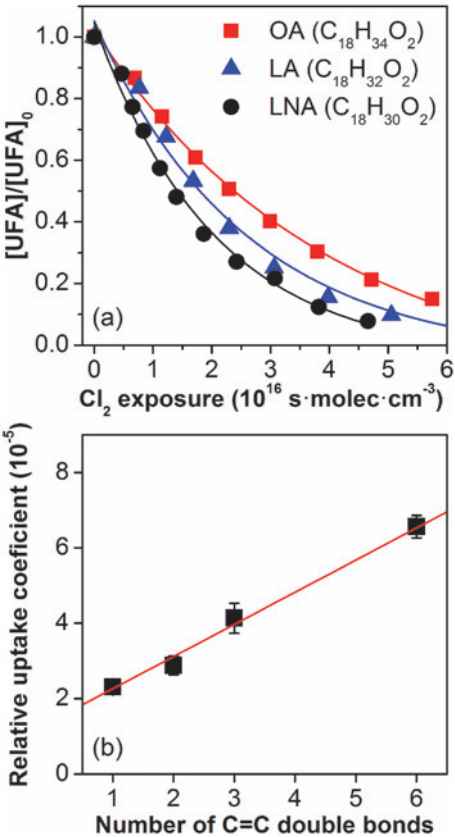

Figure 6: (a) Normalized kinetic decay of oleic acid (■), linoleic acid (▲) and linolenic acid (●) represented as a function of Cl_2 exposure. The decay curves are the fits using single exponential functions (solid lines). (b) The reactive effective uptake coefficients of unsaturated fatty acids (OA, LA and LNA) and Sqe represented as a function of the number of C=C double bonds in the molecule that compose the particles. The solid line represents a linear fit to the data.

was investigated under similar experimental conditions. Stearic acid ($C_{18}H_{36}O_2$) is a saturated fatty acid with a similar backbone structure as LNA, LA and OA, but without C=C double bonds. No reaction products are observed within the signal-to-noise of our experiment even when the Cl_2 concentration is drastically increased. This suggests that the Cl_2 molecule is unreactive towards carboxyl function groups.

As we already discussed in Section 3.1 the saturated hydrocarbon particles appear to be inert toward reaction with Cl_2 within the signal-to-noise of our experiment. In this context, the chlorination mechanism of the UFA particles by Cl_2 is proposed to be similar to the reaction mechanism proposed for chlorination of squalene particles. Thus, Cl_2 sequentially adds to the C=C double bond(s) present in the UFAs that compose the particles. Subsequently, the chlorinated UFA complexes eliminate HCl during the ionization detection. However, as in the case of squalene we cannot exclude a possible contribution from the reac-

tion of Cl_2 towards the allylic sites of UFAs once the first chlorinated products are formed.

Although the detailed mechanism for Cl_2 reactions with these three UFAs are expected to be similar, more products can be formed by those with multiple double bonds (LNA and LA) than by OA and these products may have different properties, i.e. thermal stability, ionization potential, etc.

Similar to the Sqe case, the decays in the relative intensity of the UFA ion peaks in the mass spectrum are measured as a function of Cl_2 exposure in order to determine the reactive uptake coefficient. Figure 6(a) displays the normalized decay curves for the UFAs, i.e. LNA, LA, and OA, ($[UFA]/[UFA]_0$) as a function of Cl_2 exposure. The decays of the UFA ion signals with Cl_2 exposure are fitted using an exponential function as described in Section 2.2. Solid lines in Figure 6(a) represent the fits to the experimental data.

3.3 Reactive effective uptake coefficients

The normalized decay of squalene ($[Sqe]/[Sqe]_0$), as a function of Cl_2 exposure (Figure 4a) is used to determine the effective initial reactive uptake coefficient. The decay constant, k_{Sqe} is obtained from an exponential fit to the decay trace shown in Figure 4(a). The effective reactive uptake coefficient is subsequently computed using eqn. 2 and a value of $\gamma_{Cl_2}^{Sqe} = (0.66 \pm 0.03) \times 10^{-4}$ is obtained for the Sqe reactive uptake coefficient.

The kinetic evolution of (Sqe – H)Cl, (Sqe – 2H)Cl_2, (Sqe – 3H)Cl_3 and (Sqe – 4H)Cl_4 reaction products displayed in Figure 4(b), (c), (d) and (e) are also fitted using eqn. 3 in order to approximate the rates of formation of these products relative to the reaction rate of Sqe. Equation 3 describes a sequential oxidation mechanism in a particle that is well mixed on the time scale of the reaction.

$$\frac{[(\mathrm{Sqe} - n\mathrm{H})\,\mathrm{Cl}_n]}{[\mathrm{Sqe}]_0} = B_n \cdot \frac{\left(k_{\mathrm{Sqe}} \cdot \langle \mathrm{Cl}_2 \rangle_t \cdot t\right)^n}{n!} \cdot \exp\left(k_{\mathrm{Sqe}} \cdot \langle \mathrm{Cl}_2 \rangle_t \cdot t\right) \qquad (3)$$

In eqn. (3), k_{Sqe} represents the second order heterogeneous rate constant while n denotes the product generation. For unreacted Sqe $n = 0$. B_n is an adjustable parameter to account for differences in isotope abundance, VUV photoionization efficiency, and fragmentation patterns of the oxidation products and Sqe.

The kinetics of consecutive reactions are difficult to deconvolve and for certain reactions we cannot distinguish between the reactive uptake coefficients. To approximate the reaction rates of (Sqe – H)Cl, (Sqe – 2H)Cl_2, (Sqe – 3H)Cl_3

and $(Sqe - 4H)Cl_4$ products relative to the reaction rate of Sqe, the kinetic evolution of chlorinated products is represented using a rate constant (k') that is smaller than the measured rate (k_{Sqe}) for Sqe. For simplicity, the reaction rate coefficients of first, second, third and fourth generation products of Sqe are assumed to be k'. Model fits to the $(Sqe - H)Cl$ and $(Sqe - 2H)Cl_2$, $(Sqe - 3H)Cl_3$, and $(Sqe - 4H)Cl_4$ experimental data are displayed in Figure 4(b)–(e) as solid lines. The kinetic behavior of $(Sqe - H)Cl$ and $(Sqe - 2H)Cl_2$, $(Sqe - 3H)Cl_3$, and $(Sqe - 4H)Cl_4$ is best captured by using a rate that is 30 ± 6% slower than k_{Sqe} measured for Sqe. Thus, the reaction rate coefficients are found to decrease as reaction progress.

The effective initial reactive uptake coefficients of unsaturated fatty acids, OA, LA, and LNA, were determined in a similar manner as described for the Sqe particles. Thus, the determined values of the effective reactive uptake coefficients are: $\gamma_{Cl_2}^{OA} = (0.23 \pm 0.14) \times 10^{-4}$ for OA, $\gamma_{Cl_2}^{LA} = (0.28 \pm 0.025) \times 10^{-4}$ for LA, and $\gamma_{Cl_2}^{LNA} = (0.41 \pm 0.04) \times 10^{-4}$ for LNA, respectively.

In summary, the reactive uptake coefficients of Cl_2 by the unsaturated particles, UP, (UP = squalene and unsaturated fatty acids) measured in the present work are very low, i.e. $\gamma_{Cl_2}^{UP} = 0.23 \times 10^{-4} - 0.66 \times 10^{-4}$, and are observed to increase with the increase of the number of C=C double bonds in the molecule that compose the particles. The Cl_2 + squalene reaction is observed to have the highest reactive coefficient ($\gamma_{Cl_2}^{Sqe} = (0.66 \pm 0.03) \times 10^{-4}$), which can be explained by the larger number of C=C double bonds in Sqe available for addition compared to UFAs.

The evolution of the reactive effective uptake coefficient as a function of the number of unsaturated reaction sites (1, 2, 3, and 6 for OA, LA, LNA, and Sqe, respectively) is represented in Figure 6(b). As can be seen in Figure 6(b), the reactive effective uptake coefficients are a linear function of the number of C=C double bonds present in the molecule that compose the particles. This trend is in agreement with the common knowledge of the chemical reactivity of the double bond system in the gas-phase and provides strong evidence that Cl_2 preferentially attacks the C=C double bond of these unsaturated molecules. However, this trend is in contrast to some recent studies where the reactive effective uptake coefficient of OH and NO_3 by unsaturated fatty acids has been found to be larger than the reactive effective uptake coefficient measured for Sqe [31, 32, 34].

In the case of the OH oxidation reaction, the value of the Sqe reactive effective uptake coefficient is much larger and has been found to be smaller than the one calculated in the case of LA and LNA particles. This was attributed to the differences in the reactive uptakes of OH radicals at the particle surface and particle-phase secondary reactions, and O_2 was suggested to promote chain prop-

agation in the case of OH + squalene reaction, and chain termination in the case of OH + unsaturated fatty acid reactions [31, 32].

The values of the reactive uptake coefficients for the reaction of NO_3 with unsaturated fatty acids (OA, LA, LNA) have been also reported to be higher than that measured in the case of Sqe particles [33, 34]. The larger reactive uptake coefficients measured for UFAs was attributed to either an additional contribution to the reactivity from the extra carboxylic acid functional group in unsaturated organic acids, or from secondary reactions. However, the degree of contribution from the extra carboxylic acid functional group remained unclear.

As already discussed above, the carboxylic functional group does not seem to play a role in the reaction between Cl_2 and unsaturated fatty acids particles while the contribution from secondary reaction might be small in the case of such slow reactions. Therefore we assume that the observed reaction products after the reaction between Cl_2 molecule and UFAs are exclusively due to the Cl_2 attack on the C=C double bonds present in the molecules that compose the particles. This is in agreement with some studies that report the reaction between O_3 and UFAs (OA, LA, and LNA) to proceed through an addition mechanism in which the C=C bonds of UFAs are directly attacked by the ozone molecule [35–38]. The reactive uptake coefficient of ozone with UFAs has been reported to increase with the degree of unsaturation among these three UFAs, similar to the present results. In addition, the ozonolysis of UFA particles indicated an enhanced rate of reaction compared to the analogous gas-phase reactions.

The values of the reactive effective uptake coefficient ($\sim 10^{-4}$) measured in the present study indicate that on average only one molecule is reacted in a particle per 10 000 collisions between Cl_2 molecules and the unsaturated particles. Therefore, Cl_2 molecules might diffuse within the particle instead of directly reacting with or scattering from the particle surface.

The reaction of another halogen, iodine, with squalene particles was investigated in our laboratory under similar experimental conditions. Although the I_2 molecule itself (used as photolytic precursor for I atom production) was found to be unreactive towards unsaturated squalene particles, within the signal-to-noise, the reaction of I atoms with squalene particles results in observable iodinated squalene products. Despite the fact that similar gas-phase reactions are expected to have extremely low probability, the reaction of I atoms with squalene particles has been found to take on a probability of 10^{-4} due to the trapping and consequently the multiple interactions of the I atoms into the squalene aerosol particles.

Based upon the calculated value of reacto-diffusive length (l_{RD}) of Cl_2 molecule into Sqe (l_{RD} = 76 nm), which has a value comparable to the parti-

cle radius, it is likely that the observed reaction between squalene particles and Cl_2 molecules is also due to the long time trapping of Cl_2 molecules in the particle, which considerably increases the probability of an encounter of the Cl_2 molecule with a C=C double bond. The trapping and consequently the multiple interactions of the reagents, i.e., 10 000 collisions or more, in the aerosol particles are considered also here to be the key to why chlorinated particles are formed at room temperature just in the aerosol particle and not in the gas-phase. Similarly, the reactivity of UFA particles toward Cl_2 is consequently explained based on the multiple collisions that Cl_2 experiences during the diffusion in the particle.

4 Conclusion

The heterogeneous reaction of Cl_2 molecule with particles composed of unsaturated molecules such as oleic acid, linoleic acid, linolenic acid or squalene are analyzed using an aerosol mass spectrometry technique to investigate the influence of the number of C=C double bonds in the molecule that compose the particle on the particle reactivity. All the investigated unsaturated particles are found to slowly react with Cl_2 molecules, and chlorinated molecules are formed and detected. The reactions are found to proceed by an addition mechanism in which the Cl_2 molecule attacks the C=C double bonds present in the molecules that compose the unsaturated particles. The reactive effective uptake coefficient is found to increase with the number of C=C double bonds present in the unsaturated molecule that compose the particle from $(0.23 \pm 0.01) \times 10^{-4}$ for OA, to $(0.29 \pm 0.025) \times 10^{-4}$ for LA, $(0.41 \pm 0.04) \times 10^{-4}$ for LNA and $(0.66 \pm 0.03) \times 10^{-4}$ for Sqe. The chemical evolutions of Sqe and its chlorinated products reveal that the reaction becomes slower for higher generation products. Although similar gas-phase reactions are expected to have extremely low probability, the reactions of the Cl_2 molecules with unsaturated particles composed of Sqe, LNA, LN and OA take on a probability of 10^{-4} due to the trapping and consequently the multiple interactions of the Cl_2 molecule into the unsaturated particles.

Acknowledgement: This work was supported by the Director, Office of Energy Research, Office of Basic Energy Sciences, Chemical Sciences Division of the U.S. Department of Energy under Contract No. DE-AC02-05CH11231. In particular, D. M. P.-V. is grateful to the Alexander von Humboldt Foundation for a Feodor Lynen fellowship.

References

1. S. F. Rowland, Annu. Rev. Phys. Chem. **42** (1991) 731.
2. M. J. Molina, L. T. Molina, and C. E. Kolb, Annu. Rev. Phys. Chem. **47** (1996) 327.
3. B. J. Finlayson-Pitts and J. N. Pitts, *Chemistry of the Upper and Lower Atmosphere: Theory, Experiments and Applications*, Academic Press, San Diego, CA (2000).
4. B. J. Finlayson-Pitts, Res. Chem. Intermed. **19** (1993) 235.
5. W. C. Keene, *Naturally Produced Organohalogens*, A. Grimvall and E. W. B. d. Leer, Kluwer Academic Publishers, Dordrecht (1995).
6. A. D. Keil and P. B. Shepson, J. Geophys. Res. **111** (2006) D17303.
7. P. J. Tackett, A. E. Cavender, A. D. Keil, P. B. Shepson, J. W. Bottenheim, S. Morin, J. Deary, A. Steffen, and C. Doerge, J. Geophys. Res. **112** (2007) D07306.
8. C. W. Spicer, E. G. Chapman, B. J. Finlayson-Pitts, R. A. Plastridge, J. M. Hubbe, J. D. Fast, and C. M. Berkowitz, Nature **394** (1998) 353.
9. M. J. Lawler, R. Sander, L. J. Carpenter, J. D. Lee, R. v. Glasow, R. Sommariva, and E. S. Saltzman, Atmos. Chem. Phys. **11** (2011) 7617.
10. J. Liao, L. G. Huey, Z. Liu, D. J. Tanner, C. A. Cantrell, J. J. Orlando, F. M. Flocke, P. B. Shepson, A. J. Weinheimer, S. R. Hall, K. Ullmann, H. J. Beine, Y. Wang, E. D. Ingall, C. R. Stephens, R. S. Hornbrook, E. C. Apel, D. Riemer, A. Fried, R. L. Mauldin III, J. N. Smith, R. M. Staebler, J. A. Neuman, and J. B. Nowak, Nature Geosci. **7** (2014) 91.
11. T. P. Riedel, T. H. Bertram, T. A. Crisp, E. J. Williams, B. M. Lerner, A. Vlasenko, S.-M. Li, J. Gilman, J. d. Gouw, D. M. Bon, N. L. Wagner, S. S. Brown, and J. A. Thornton, Environ. Sci. Technol. **46** (2012) 10463.
12. P. L. Tanaka, S. Oldfield, J. D. Neece, C. B. Mullins, and D. T. Allen, Environ. Sci. Technol. **34** (2000) 4470.
13. J. M. Roberts, H. D. Osthoff, S. S. Brown, and A. R. Ravishankara, Science **321** (2008) 1059.
14. R. Vogt, P. J. Crutzen, and R. Sander, Nature **383** (1996) 327.
15. E. M. Knipping, M. J. Lakin, K. L. Foster, P. Jungwirth, D. J. Tobias, R. B. Gerber, D. Dabdub, and B. J. Finlayson-Pitts, Science **288** (2000) 301.
16. M. E. Gebel and B. J. Finlayson-Pitts, J. Phys. Chem. A **105** (2001) 5178.
17. A. Laskin, D. J. Gaspar, W. H. Wang, S. W. Hunt, J. P. Cowin, S. D. Colson, and B. J. Finlayson-Pitts, Science **301** (2003) 340.
18. G. Deiber, C. George, S. L. Calve, F. Schweitzer, and P. Mirabel, Atmos. Chem. Phys. **4** (2004) 1291.
19. M. Kanakidou, J. H. Seinfeld, S. N. Pandis, R. Barnes, F. J. Dentener, M. C. Facchini, R. v. Dingenen, B. Ervens, A. Nenes, C. J. Nielsen, E. Swietlicki, J. P. Putaud, Y. Balkanski, S. Fuzzi, J. Horth, G. K. Moortgat, R. Winterhalter, C. E. L. Myhre, K. Tsigaridis, E. Vignati, E. G. Stephanou, and J. Wilson, Atmos. Chem. Phys. **5** (2005) 1053.
20. W. A. Lonneman, R. L. Seila, and S. A. Meeks, Environ. Sci. Technol. **20** (1986) 790.
21. R. B. Zweidinger, J. E. Sigsby, S. B. Tejada, F. D. Stump, D. L. Dropkin, W. D. Ray, and J. W. Duncan, Environ. Sci. Technol. **22** (1988) 956.
22. S. Sawada and T. Totsuka, Environ. Sci. Technol. **20** (1986) 821.
23. W. F. Rogge, L. M. Hildemann, M. A. Mazurek, G. R. Cass, and B. R. T. Simoneit, Environ. Sci. Technol. **25** (1991) 1112.
24. W. F. Rogge, L. M. Hildemann, M. A. Mazurek, G. R. Cass, and B. R. T. Simoneit, Environ. Sci. Technol. **27** (1993) 1892.

25. J. March, *Advanced Organic Chemistry: Reactions, Mechanisms, and Structure*, 4th edn., Wiley, New York (1992).
26. F. Asinger, *Mono-Olefins: Chemistry and Technology*, Pergamon Press Ltd, Oxford (1968).
27. H. P. A. Groll, G. Hearne, F. F. Rust, and W. E. Vaughan, Ind. Eng. Chem. **31** (1939) 1239.
28. F. Freeman, Chem. Rev. **75** (1975) 439.
29. J. D. Graham and J. T. Roberts, J. Phys. Chem. B. **104** (2000) 978.
30. T. Moise and Y. Rudich, Geophys. Res. Lett. **28** (2001) 4083.
31. T. Nah, S. H. Kessler, K. E. Daumit, J. H. Kroll, S. R. Leone, and K. R. Wilson, Phys. Chem. Chem. Phys. **15** (2013) 18649.
32. T. Nah, S. H. Kessler, K. E. Daumit, J. H. Kroll, S. R. Leone, and K. R. Wilson, J. Phys. Chem. A **118** (2014) 4106.
33. Z. Zhao, S. Husainy, C. T. Stoudemayer, and G. D. Smith, Phys. Chem. Chem. Phys. **12** (2011) 17809.
34. L. Lee, P. Wooldridge, T. Nah, K. R. Wilson, and R. Cohen, Phys. Chem. Chem. Phys. **15** (2013) 882.
35. T. Moise and Y. Rudich, J. Phys. Chem. A **106** (2002) 6469.
36. J. W. Morris, P. Davidovits, J. T. Jayne, J. L. Jimenez, Q. Shi, C. E. Kolb, D. R. Worsnop, W. S. Barney, and G. Cass, Geophys. Res. Lett. **29** (2002) 71-1.
37. J. D. Hearn and G. D. Smith, J. Phys. Chem. A **108** (2004) 10019.
38. T. Thornberry and J. P. D. Abbatt, Phys. Chem. Chem. Phys. **6** (2004) 84.
39. D. M. Popolan-Vaida, K. R. Wilson, and S. R. Leone, J. Phys. Chem. A **118** (2014) 10688.
40. J. D. Smith, J. H. Kroll, C. D. Cappa, D. L. Che, C. L. Liu, M. Ahmed, S. R. Leone, D. R. Worsnop, and K. R. Wilson, Atmos. Chem. Phys. **9** (2009) 3209.
41. C.-L. Liu, J. D. Smith, D. L. Che, M. Ahmed, S. R. Leone, and K. R. Wilson, Phys. Chem. Chem. Phys. **13** (2011) 8993.
42. D. W. Berman, V. Anicich, and J. L. Beauchamp, J. Am. Chem. Soc. **101** (1979) 1239.
43. Webbook, The National Institute of Standards and Technology (NIST) Gaithersburg, MD.